Motions and Relaxations of Confined Liquids

Steve Granick

Motions and Relaxations of Confined Liquids

STEVE GRANICK

When a liquid is confined in a narrow gap (as near a cell membrane, in a lubricated contact between solids, or in a porous medium), new dynamic behavior emerges. The effective shear viscosity is enhanced compared to the bulk, relaxation times are prolonged, and nonlinear responses set in at lower shear rates. These effects are more prominent, the thinner the liquid film. They appear to be the manifestation of collective motions. The flow of liquids under extreme confinement cannot be understood simply by intuitive extrapolation of bulk properties. Practical consequences are possible in areas from tribology and materials processing to membrane physics.

CONSIDER THE ARMCHAIR EXPERIMENT DEPICTED IN FIG. 1. Take a drop of liquid, put it between a ball and a table—and let the ball fall. Of course the liquid squirts out, initially rapidly, then slower and slower as the liquid thickness becomes less than the radius of the ball. This problem was solved more than 100 years ago in a classic analysis of Reynolds (1). Experimentally, Israelachvili and co-workers showed that the film eventually stabilizes at a finite thickness of a few molecular diameters (2, 3). The liquid film supports the weight of the ball! An extraordinarily large pressure is needed to squeeze out the final few layers of liquid between two solid surfaces. Why?

Liquids tend to organize in strata parallel to a solid boundary, provided that the boundary is smooth compared to the molecular size. A density profile for a liquid of spherical particles is shown schematically in Fig. 2. The mean local density of liquid is plotted against the distance between two solid boundaries. The graph is analogous to the well-known radial distribution function that describes the order around an average molecule in an isotropic liquid (4). Close to the boundaries, the liquid density is vanishingly low because no particle can be located precisely there, but the local density is correspondingly large at a distance of one particle radius removed, while again it reaches a minimum one further particle radius away, and so forth. This density wave typically propagates outward for a distance of three to ten particle dimensions. In the situation depicted in Fig. 1, the liquid supports the weight of the ball when the interfacial regions depicted in Fig. 2 begin to overlap. This much is well understood in principle (5, 6).

But what is the organization in directions parallel to the surfaces? Because surfaces extend laterally over macroscopic distances, there are opportunities for interesting degrees of order or disorder in the direction tangent to the surfaces. This fundamental difference from the bulk liquid, which has only recently been investigated (7–14), is discussed below.

Apart from questions of structure, what are the dynamics of liquids in intimate contact with a solid boundary? This question has

proven to be one of the most baffling aspects of liquids, in spite of long-standing interest (15, 16).

Rapid advances are now being made with the advent of new experimental tools. The author's intention in writing a review at this time is to bring out the excitement of a field that is in the throes of rapid development.

Flow of Confined Liquids

Basic principles. Neglecting surface effects for the moment, recall that liquids can be distinguished from solids as sustaining no deformation at equilibrium. In responding to force, a liquid eases deformation by flowing at some rate. Shear deformation, in which one surface slides tangent to another, is especially simple to interpret. At sufficiently low shear rates (shear rate equals velocity divided by film thickness), flow obeys Newton's law,

$$\sigma = \eta \, d\gamma/dt \qquad (1)$$

where σ is the shear stress (stress is the force divided by area), $d\gamma/dt$ is the shear rate ($\dot{\gamma}$), and η is the viscosity, which has dimensions of mass length^{-1} time^{-1}. A conventional unit is the poise (cgs units). The range of liquid viscosities is enormous. At room temperature the viscosities of water, honey, and road tar are approximately 0.01, 10, and 10^{10} poise, respectively. The viscosity of a liquid may be thought of qualitatively as its resistance to flow.

These notions become more subtle when the liquid film is so thin as to be anisotropsurfaces. An example may be seen in Fig. 1; after the ball has fallen, the ic in the directions normal to and parallel to
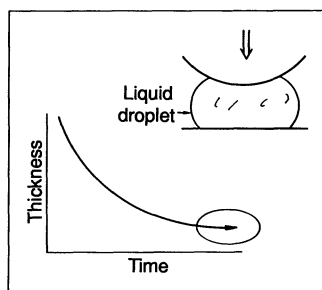
Fig. 1. Hypothetical experiment showing that a liquid can support a normal force. A liquid droplet is placed between a ball and a flat surface. The graph, in which liquid thickness is plotted schematically against time after the ball has begun to fall, shows that the film thickness remains finite (a few molecular dimensions), even at equilibrium.

Fig. 2. Schematic diagram of the local density of a liquid of spherical particles, plotted against the distance between two solid boundaries. The tendency to order in layers parallel to the boundaries is indicated by decaying oscillations with a period of about a particle diameter. This differs from the radial distribution function of a bulk liquid in the sense that interesting degrees of order and disorder parallel to the boundary are also possible.
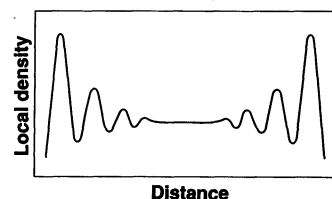
The author is in the Materials Research Laboratory and Department of Materials Science and Engineering, University of Illinois, Urbana, IL 61801.

the ultrathin liquid supports an equilibrium normal force. It acts as a solid in this direction.

What of sliding of one surface tangent to another? Long ago, it was recognized that it takes more force to squeeze a liquid out of a confined space than it does to shear the film (17). When dealing with an ultrathin film, analysis shows that if local viscosity coefficients could be measured, they would vary with distance across a thin liquid film just as the local density does (18–20). A laboratory shear experiment averages over the width of the film. Nonetheless it is meaningful to define an effective viscosity based on Eq. 1. However, when a liquid film is sufficiently thin, its response to a tangential force is that of a solid. Then one measures rigidity or yield stress.

What determines the effective viscosity of a film that is so thin? What makes ultrathin liquids turn solid when they are sufficiently thin? Why is solidification suppressed by continuous motion? These are key problems in this area.

Measuring the flow of ultrathin liquid films. The experimental approach is to confine a liquid between two parallel plates of single crystals whose area is vast compared to the thickness between them. This is an ideal condition in which to study flow behavior because it allows one to produce liquid films whose thickness is defined down to a resolution of an angstrom—less than the thickness of a single molecule!

The various instruments that have been devised to do this (21–25) are extensions of the surface forces apparatus (26, 27). The surface forces apparatus has been described in detail (26, 27). In brief, liquid is confined between two crystals (usually of muscovite mica or thin films of other materials coated onto muscovite mica) oriented as cylinders at right angles to one another. The distance between the surfaces can be controlled from thousands of angstroms down to molecular dimensions.

The innovation to measure shear flow is based on having parallel plate (rather than crossed cylinder) geometry. As the smoothly curved solid sheets are brought close together, the liquid in the final few molecular layers resists being squeezed out. A soft glue placed under the mica sheets flattens instead, resulting in a circular area of closest approach on each sheet. Optical interferometry of the surface separation and of the surface contour confirms that the two flattened zones are parallel and provides the contact diameter. The diameter of the flattened area (on the order of 10^5 Å) is vast compared with the thickness of the confined liquid.

With this approach, my laboratory has studied viscous dissipation and elasticity of confined liquids by using periodic sinusoidal oscillations over a range of amplitudes and frequencies (24, 25, 28–33). The geometry of the shear deformation is illustrated in Fig. 3. Other workers have used a different apparatus to study the friction encountered during sliding at a constant speed (23, 34–38). Early measurements involved dry sliding (21, 22, 39). The technical difficulties of these methods have been discussed elsewhere (40).

Effective Viscosity of a Simple, Confined Molecular Liquid

Every liquid that has been investigated [a variety of nonpolar liquids of various sizes, shapes, and flexibilities (24, 28–33)] shows the following qualitative effects, but findings for dodecane are emphasized in this article for illustration.

Dodecane, $CH_3(CH_2)_{10}CH_3$, is a simple flexible chain molecule 12 carbons long. Its bulk shear viscosity at room temperature is 0.01 poise, independent of shear rate up to shear rates $>10^{10}$ s^{-1}. The chain length is $\sim$18 Å, and the thickness of the chain is $\sim$4 Å. The static structure of chains of similar length, confined between parallel plates, has been simulated by computer (41, 42).

As mica cylinders separated by a dodecane droplet are pushed

Fig. 3. Schematic diagram illustration periodic shear deformation. The word "shear" signifies sliding of one body parallel to another. The arrow denotes the shear direction.
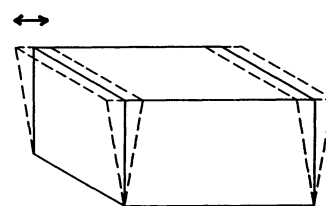
together, fluid drains smoothly until, at a thickness of $\sim$50 Å, equilibrium normal forces of alternate attraction and repulsion set in as successive liquid layers are pushed out (3, 32). These are manifestations of the inhomogeneous density profile illustrated in Fig. 2. The period of oscillation of the forces is the width of a methylene segment, $\sim$4 Å, showing that molecules are aligned preferentially parallel to the boundaries. An interesting consequence of the oscillatory profile of force versus distance is that the same normal force is satisfied by several values of the film thickness; therefore, the profile measured in any particular experiment is ultrasensitive to experimental details, such as the rate at which the liquid droplet is squeezed down to a particular distance (24, 29). In Fig. 1, there are multiple solutions for the film thickness at which a ball would stop falling.

Linear response. Shear viscosity depends on film thickness. In the region of inhomogeneous density in Fig. 1, the effective viscosity is larger than in the bulk and grows with diminishing thickness. In Fig. 4, the limiting effective viscosity at low shear rate calculated with Eq. 1, η°_{eff}, is plotted against film thickness. In this experiment, the crossed cylinders first flattened to form parallel plates at film thickness of $\sim$40 Å, and therefore this is the first point at which shear measurements were made. The effective viscosity was already greater than in the bulk. Drainage to lesser thickness was caused by applying additional net normal pressure. The four data points at the least thickness (26 ± 1 Å) all refer to a film of approximately six segmental widths. The adjustments of thickness by 1 to 2 Å with increasing net normal pressure, less than the segmental width, reflect compressibility of the liquid. The effective viscosity seems to diverge.

Nonlinear response. The simple flow properties of dodecane in a beaker turn complex when dodecane is confined. The essentially nonlinear shear response under confinement is illustrated in Fig. 5. The data refer to a film of thickness 27 Å at a modest net normal pressure (0.12 MPa; $\sim$1.2 atm). The maximum viscous force during a cycle of oscillation (f_{max}) is plotted against the maximum velocity (v_{max}).

Two immediate conclusions follow from the data in Fig. 5. First, f_{max} grew in direct proportion to v_{max} at sufficiently low values, but beyond a modest velocity (400 Å s^{-1}) it grew more slowly. Second, the data show that the reducing variable by which to analyze the viscous force was indeed velocity, not frequency (43) as at smaller strains. This follows because when amplitude and frequency were varied separately, the viscous force depended only on their product.

The characteristic length of this flow problem may safely be taken
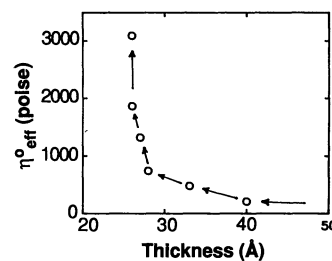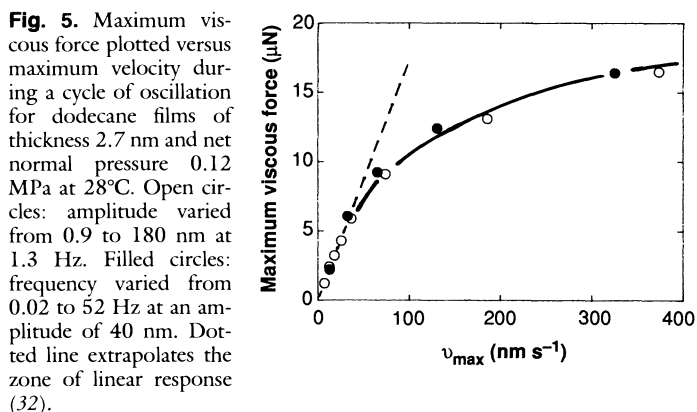

Fig. 4. Effective limiting viscosity at low shear rate, plotted against film thickness, for confined dodecane films at 28°C. Arrows indicate direction of increasing compression.

Fig. 5. Maximum viscous force plotted versus maximum velocity during a cycle of oscillation for dodecane films of thickness 2.7 nm and net normal pressure 0.12 MPa at 28°C. Open circles: amplitude varied from 0.9 to 180 nm at 1.3 Hz. Filled circles: frequency varied from 0.02 to 52 Hz at an amplitude of 40 nm. Dotted line extrapolates the zone of linear response (*32*).

[Graph: Maximum viscous force (μN) vs v_{max} (nm s^{-1})]

by viscous dissipation, straightforward calculation shows that it was efficiently dissipated because the area of the films was so large relative to the thickness. Even cursory inspection of raw data such as in Fig. 5 shows these effects; they do not depend on analyzing the data in terms of an effective viscosity. While the characteristic length by which to normalize the velocity might be somewhat less than the total film thickness [one or two layers of fluid might be pinned to each surface during the experiment (*13, 16, 44*)], such fine-tuning of the analysis would not change the relative numbers analyzed above, nor their orders of magnitude. The consistent measurements obtained in repeated experiments with different liquids would indicate that the results are general and must be examined at face value.

Discussion

Measurements at large deformation. It is at first astonishing to scientists who study the flow of liquids that the data depend on velocity rather than on the excitation frequency. One is not accustomed to this (*43*). However, the strains customarily investigated (strain is shear amplitude divided by film thickness) are on the order of unity or less. The strains reported here are enormously larger—15 for the constant amplitude experiments in Fig. 5.

In fact, a tendency for frequency and amplitude shear data to converge at large strains was already observed long ago in studies of bulk flow (*45*). The matter has been relatively neglected since then. Ferry has suggested as a rough qualitative interpretation that an experiment performed with sinusoidal oscillations of huge amplitude relative to the film thickness is really more like a steady-flow experiment, with shear rate averaged over a cycle (*46*). In other words, most of the plot in Fig. 5 is essentially a non-Newtonian flow plot.

Enhanced viscosity and slow relaxation. Physically, a nonlinear viscosity sets in when the experiment distorts the structure of the fluid. This happens when the experimental time scale is faster than a characteristic time of Brownian motion. In Fig. 6, the onset of nonlinear response is readily estimated by extrapolating the plateau and power-law zones until they cross. The conclusion that the nonlinear response sets in at $\dot{\gamma}_{eff} > 20$ s^{-1} for dodecane implies that the longest system relaxation time was $\sim 1/20 = 0.05$ s—more than 10^8 times slower than in the bulk. This is a central theme: relaxation is much slower than in the bulk liquid.

Further insight into the molecular origin of slow relaxation comes when one calculates, from the rate of increase in η_{eff} with increasing net normal pressure, the activation volume (ΔV_{act}) for flow (*32*). The finding is that ΔV_{act} is tremendously larger than for flow in the bulk. In the zone of linear viscous response, the activation volume corresponds to the volume of ~ 200 molecules; this stands in sharp contrast to diffusion in the bulk liquid, where ΔV_{act} amounts to the volume of only a single segment of the molecule (*47*). However, under confinement, ΔV_{act} decreases with increasing $\dot{\gamma}_{eff}$ in the zone of nonlinear response (*32*). These findings indicate that the unit event in shear flow was collective and that shear thinning involved the breaking up of some structure. The activation volume in the zone of linear response is an estimate of the correlated volume that exists even in the absence of flow.

Explanations are still conjectural. If collective motions are responsible for the high viscosity and slow relaxation, this might still be consistent with rapid motion of individual molecules. Indeed, the existing computer simulations of confined liquids indicate that the diffusion of spherical molecules is only moderately slowed down by confinement (see critical discussion below). The problem then becomes to understand the origin of collective motions and how they might be broken up by externally driven flow.

to be the thickness of the liquid film (other conceivable length scales have similar magnitude; see below). For the same set of data shown in Fig. 5, Fig. 6 shows the effective viscosity (η_{eff}) calculated with Eq. 1, plotted against maximum effective shear rate ($\dot{\gamma}_{eff}$) on log-log scales in view of the large changes in magnitude. At low shear rate, η_{eff} was constant. As the shear rate increased, extensive decrease of η_{eff} occurred. The rate of this shear thinning followed an empirical power law, $\eta_{eff} \sim \dot{\gamma}_{eff}^{-a}$. The power a, always slightly more than two-thirds, was not quite constant; at a given film thickness it increased modestly with increasing net normal pressure (*32*), tending toward unity for the thinnest films (*33*).

The effective viscosity always exceeded the viscosity of bulk dodecane, but decayed by a factor greater than 100 as the shear rate was raised. Measurements of film thickness failed to detect any changes with shear (<1 Å); this puts an upper limit of 4% on possible shear-induced changes in the mean liquid density. Measurements were reversible when the velocity was raised and lowered.

This pattern of flow behavior is also characteristic of other simple nonpolar liquids. For illustration, also shown in Fig. 6 is an experiment with OMCTS, octamethylcyclotetrasiloxane, a silicone oil of different chemical shape as well as chemical composition. For some years, OMCTS, $[Si(CH_3)_2-O-]_4$, a compact-shaped (but flexible) ring molecule with diameter ~ 9 Å has been a reference liquid in studies of liquid microstructure (*2, 5*). The stronger intensity of interaction with the surface and the different molecular packing probably account for the different quantitative response as compared to dodecane; a detailed discussion is not warranted at this time. For the present we emphasize the qualitative agreement. The effective viscosity was controlled by the velocity or normalized velocity of the experiment and again showed extensive shear thinning. Thus this pattern of behavior held even for a molecule that is not a linear chain.

What of conceivable artifacts? The observation of reversibility rules out shear-induced chemical degradation. As for heat generated
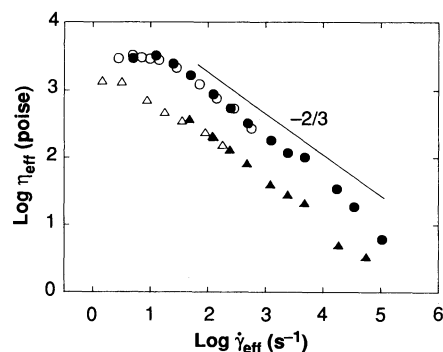
[Graph: Log η_{eff} (poise) vs Log $\dot{\gamma}_{eff}$ (s^{-1}), with line labeled −2/3]

Fig. 6. Double logarithmic graph of effective viscosity as a function of strain rate. Circles: dodecane film specified in Fig. 4. Triangles: OMCTS film of thickness 2.7 nm and net normal pressure 0.14 MPa. Open symbols: amplitude varied at constant frequency. Filled symbols: frequency varied at constant amplitude (*32*).

If this were a strictly two-dimensional (2-D) fluid, then long-time tails of velocity correlations resulting from hydrodynamics could come into play, leading to divergence of the 2-D shear viscosity at low frequency (4, 48) and its logarithmic decay with increasing shear rate (49). However, the deformation in these experiments was not applied within a 2-D plane. Moreover, long-time hydrodynamic tails are not expected to be prominent at high density (50) as in the present experiments. Alternatively, long-lived orientational correlations (51) or density fluctuations (52) could arise because a state of two dimensions is approached. In fact, the finding that $\eta_{\rm eff} \sim \dot\gamma_{\rm eff}^{-2/3}$ is predicted by a cluster model of shear thinning (52). A provocative recent scanning tunneling microscopy (STM) study of alkanes at the liquid-graphite surface suggests that microcrystalline domains actually form in the monolayer immediately at the surface (53). Further investigations are needed to clarify these striking effects. A problem in assessing 2-D explanations is that rigorous predictions for systems that are close to—but not quite—in two dimensions remain to be worked out.

Solidification

When it is sufficiently thin, a confined liquid solidifies, in the sense that it will not allow shear until a critical shear stress (yield stress) is exceeded. This occurs especially for films less than four molecular dimensions thick (23, 24, 28–31, 34–38). It is tempting to attribute the phenomenon simply to strong adsorption. However, even when the overall response is liquid (four to ten molecular dimensions), the response can have an elastic component in addition to a viscous component (32, 33). This suggests that the transition to solidification, with decreasing film thickness, could be continuous.

Perhaps the parallels to what happens when gases condense onto solids are not widely enough appreciated. Condensation of noble gases on graphite is well studied (54). Theoretical understanding of the origin of the solid and liquid monolayer phases that form—commensurate or incommensurate with the underlying solid—is well developed (54). The present case is decidedly more complicated, of course, not only by the effects of externally driven motion, but also by the complicated molecules and substrates that are of concern. In future studies, ideas in these two fields of investigation, which arose independently, hopefully may stimulate one another.

Molecular interpretations of the solidification phenomenon are controversial and may remain so until the molecular packing is measured directly. Such experiments would be difficult for reasons discussed below. However, the experimental situation is simpler than might be feared. One might imagine that the state of an ultrathin film might depend on everything conceivable—especially the direction of shear relative to crystalline lattices of the solid boundaries and the relative orientation of these two crystalline lattices. The search for universal behavior would be a lost cause. Indeed, this may be so for the very thinnest films (34), but fortunately not when the film thickness is larger.

What is presently understood about solidification can be briefly summarized. First, for the very thinnest films, the yield stress increases with diminishing film thickness (23). Such yield stress behavior is a familiar fact of life, static friction. However, solidification is suppressed by continuous shear (23, 24, 28–38), as occurs in dynamic friction.

Second, computer simulations show that a liquid of spherical particles tends to crystallize epitaxially at a solid surface. The crystalline layers, typically one or two particle diameters thick (7, 10–14), can be torn apart and kept disordered by shear (13, 14). The inference is that the transition from static to dynamic friction with increasing shear force could reflect shear-induced melting. Agree-

ment with laboratory experiments has been asserted (13).

However, the solidification phenomenon is general. It is observed for every liquid investigated (23, 24, 28–30, 33–38). In particular, control experiments show that the ability of material to form bulk crystals is not necessary. A glass-forming liquid (atactic polyphenyl-methylsiloxane; glass transition temperature −20°C) also solidifies (28).

Finally, the yield stress depends strongly on experimental history (28, 29). The film thickness at solidification depends on the rate at which the liquid drop is thinned (29). The yield stress grows over remarkably long times—minutes to hours, depending on the liquid (28, 29). This strengthening can be seen in an experiment with OMCTS (Fig. 7). The yield stress on first measurement was ~3.5 MPa, but this value nearly tripled over a 10-min interval. The sluggish increases in the yield stress imply that whatever the structure may be of the solidified state, apparently it is full of defects.

The following picture has been proposed tentatively (28, 29). As discussed above, collective motions appear to be responsible for the high viscosity and slow relaxation under confinement. Increasing confinement may slow down the relaxation to the point that, finally, flow must be mechanically activated over the time scale of an experiment.

This idea of mechanical activation is consistent with the magnitude of the yield stress; interpreted as an energy density, the yield stress is in the range of 0.3 to 1 kT per molecule (28) (k is Boltzmann's constant and T is the absolute temperature). If one accepts the rule of thumb that the yield stress is on the order of 0.01 to 0.1 times the shear modulus, the estimated shear modulus resembles that of bulk glasses. Loss of fluidity may reflect vitrification imposed by the liquid's confinement.

Roles of Surface Composition and Structure

Until recently the alarming possibility existed that all of these findings might be specific to mica as the solid boundary. There were good reasons to use mica, which forms a transparent single crystal free of steps over a large area, but the question remained of what would happen if the surface lacked long-range periodicity and adsorption were weaker.

Recently methods were developed to blanket mica with a securely attached, self-assembled organic monolayer (55, 56). The surface composition, composed of chemically reacted octadecylsilane (OTE) chains, is an array of closely packed methyl groups. The methyl groups are amorphous over distances greater than 100 Å in films of this type (57); liquids could not crystallize epitaxially onto these monolayers. In addition, the surface energy is only 22 mJ m^{-2} (56), considerably less than that of freshly cleaved mica (200 to 400 mJ m^{-2}); liquids are expected to adsorb more weakly than onto mica. Thus, substantially weaker coupling to the surface is expected than in the case of mica.
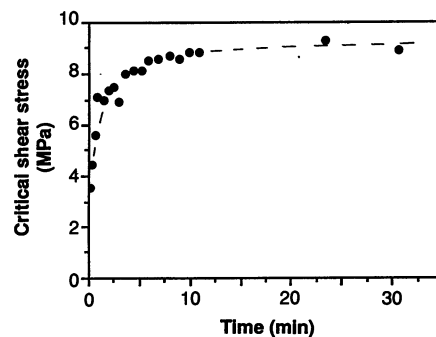

Fig. 7. Yield stress of octamethylcyclotetrasiloxane (OMCTS) plotted against elapsed time during repetitive cycles of oscillation at 1.3 Hz and at 23°C. Film thickness was 9 Å, and net normal pressure was 0.8 MPa (28).

Fundamentally the same shear viscosity was observed for dodecane confined between OTE layers (Fig. 8) as obtained with mica. The thickness of dodecane is 32 Å. Once again, effective viscosity, η_{eff} is plotted against maximum effective shear rate, $\dot{\gamma}_{eff}$, on logarithmic axes. Despite quantitative differences from the situation with mica, in both cases η_{eff} was much greater than in the bulk and decreased by a factor greater than 100 as $\dot{\gamma}_{eff}$ increased. These experiments show that the behavior described above resulted essentially from geometrical confinement.

Other Probes of Surface Dynamics

The difficulty in studying the solid-liquid interface is that it is buried between two bulk phases and that there is so little material there to study. It takes only $\sim 1 \times 10^{-7}$ g cm^{-2} of organic liquid to form a monolayer. Therefore, experiments with the sensitivity to measure dynamics are few.

When two crossed cylinders of mica are squeezed together, an effective viscosity can be inferred from the rate at which the fluid drains out (58–60). Results can be interpreted as if one or two layers of fluid molecules are immobilized on each surface on the time scale of the experiment (58, 61), which is consistent with the findings described above. The spectacular enhancement of viscosity described above is not observed, however (58, 59). The essential physical differences may be that the film thickness in those experiments was many times larger than in the shear experiments described above. If so, the different findings emphasize the extreme consequences for dynamics when fluid is confined within a narrow gap.

In another experimental approach, liquids have been confined within porous glasses in order to increase the surface area monitored by the experiment. In this curved geometry, the melting temperature and the glass transition temperature are lower than in the bulk, not higher as in a planar geometry; the reasons are still not completely understood, especially with regard to the shift in the glass transition temperature (62, 63). In view of these differences in molecular packing, how liquid dynamics measured in a porous medium relates to liquid dynamics in a planar geometry is not yet clear conceptually.

Rapid developments are expected based on spectroscopic methods, which have been used so far by only a few workers. Nuclear magnetic resonance (NMR) measurements of hydrocarbon mobility in zeolites show that the rates of conformational changes are significantly slower than in the bulk (64). Picosecond measurements of reorientation times support this, showing moderately slower relaxation times (by a factor of 3) when a polar molecule (nitroben-

zene) adsorbs to porous glass (65). However these differences disappear for a nonpolar liquid or if the glass is treated to be nonpolar (65). In fact, reorientation of supercooled oxygen in porous glass is actually faster in small pores (22 Å diameter) than in larger pores (66, 67). Greater restrictions on thermodynamic fluctuations in the smaller pores were invoked to explain this paradoxical finding (66, 67).

Very recently, evidence was found (68) that diffusion in ultra-small pores is of the form expected in a 2-D geometry (4, 69, 70). Analysis of deuteron relaxation rates measured by NMR showed that dipole-dipole correlations persist to considerably longer times in small pores (down to 34 Å diameter) than they do in the bulk (68). With increasing pore size, the transition from 2-D to 3-D relaxation was also inferred (68, 71). Extensions of these studies may allow one to set criteria for when a particular physical system is truly 2-D.

The other major approach at present is simulation by computer. Phenomena can be simulated that would be impossible to measure experimentally—for example, the trajectories and positions of individual molecules as a function of their positions in the liquid film. Indeed, most of what is known explicitly about equilibrium liquid structure at the solid-liquid interface comes from simulations (6–14). Results have begun to emerge regarding diffusion and flow of spherical particles (liquid argon) in planar confined geometries. The diffusion rates parallel to the surfaces are found to be retarded relative to the bulk, but only weakly (18–20, 44, 72, 73). As noted above, this could be reconciled with experiments if the relaxation time that controls the diffusion of individual particles is not the same as controls the viscous response.
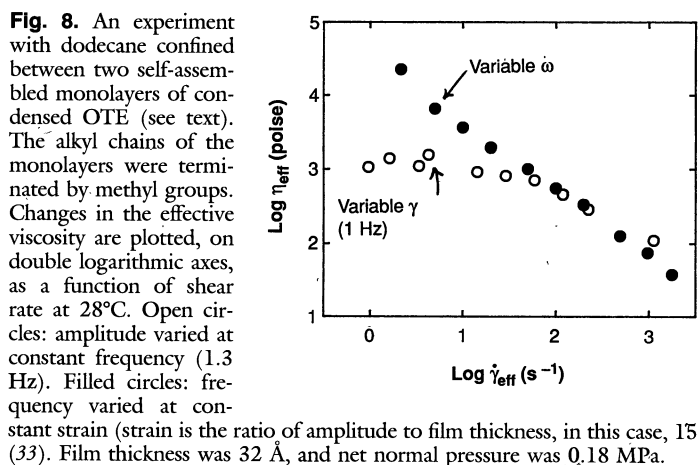
Computations about dynamics are so time-consuming, however, that the longest relaxation time that can be studied with present computers is only $\sim 1 \times 10^{-7}$ s. In order to exceed the rate of thermal motion, the lowest rate of externally driven flow that can be studied is $\sim 10^{10}$ s^{-1}. Closer comparison with experiments should be possible when the systems that can be modeled are large enough to look for the collective relaxation effects suggested above.

Future Directions

One of the most baffling aspects of liquids has long been the solid-liquid interface, despite its practical importance in areas such as friction and lubrication, flow of colloidal particles past one another, liquids in porous geological formations, the wall-stick boundary condition of classical continuum hydrodynamics, and many materials processing operations. In all of these situations the order imposed by the surface contends with the usual isotropy of the liquid, and the thermodynamic state depends not only in the usual fashion on temperature and pressure, but also on the strength of surface-fluid interactions.

One reason for slow progress is simply that liquids in the bulk were traditionally studied by chemical physicists, while liquids at surfaces were studied by engineers. There was little interaction between these communities and their common problems tended to be neglected. Another reason is the paucity of experimental methods with which to probe this interface that is buried between two condensed phases. This is starting to change with the advent of new experimental tools. The preceding account has necessarily been limited to a few examples. The field is developing rapidly. Presently it is poised at the stage where a growing body of data is begging for definitive explanation.

The patterns described in this article appear to be general, but the magnitudes likely depend on particular properties of the liquid (the molecular size, shape, polarity, and chemical composition), as well

Fig. 8. An experiment with dodecane confined between two self-assembled monolayers of condensed OTE (see text). The alkyl chains of the monolayers were terminated by methyl groups. Changes in the effective viscosity are plotted, on double logarithmic axes, as a function of shear rate at 28°C. Open circles: amplitude varied at constant frequency (1.3 Hz). Filled circles: frequency varied at constant strain (strain is the ratio of amplitude to film thickness, in this case, 15 (33). Film thickness was 32 Å, and net normal pressure was 0.18 MPa.

as on the strength of surface-fluid attraction. This has been considered based on general statistical mechanical considerations (6), but system-specific chemical effects are still poorly understood.

This interdisciplinary area should be greatly stimulated as more theorists seek to explain the data that has accumulated. Contact is waiting to be made with modern ideas of liquid-state physics, wetting phenomena, and systems trapped far from equilibrium.

Other progress is likely with new experimental techniques. The potential of spectroscopic and diffraction investigations has been emphasized. New experimental approaches are needed to resolve the questions raised above of shear ordering and disordering.

The approaches emphasized in this article also apply to more complicated liquids. For example, liquids of highly intertwined polymer chains exhibit more prominent elasticity—while still remaining liquid—than they do in the bulk (33). Fluid mixtures [containing, for example, polymers (74), block copolymers, detergents, and proteins] and aqueous media are also obvious next steps.

The question of biological systems is open. A tantalizing hint of connections to be made with membrane physics is suggested by the experiments, discussed above (Fig. 8), in which the solid boundary consisted of hydrocarbon chains. Of course, only the simplest nonpolar liquids have been studied to date. In broaching the behavior of water, especially of water close to proteins, nucleic acids, and membranes, experiments in which solid organic surfaces of tailored chemical composition are used may result in direct biological implications.

REFERENCES AND NOTES

1. O. Reynolds, *Trans. Roy. Soc.* **177** (Part 1) **1886**, 157 (1886).
2. R. G. Horn and J. N. Israelachvili, *J. Chem. Phys.* **75**, 1400 (1981).
3. H. K. Christenson, D. W. R. Gruen, R. G. Horn, J. N. Israelachvili, *ibid.* **87**, 1834 (1987), and references therein.
4. For a review, see J.-P. Hansen and I. R. McDonald, *Theory of Simple Liquids* (Academic Press, New York, ed. 2, 1986).
5. For a review of experiments, see H. K. Christenson, *J. Dispersion Sci. Technol.* **9**, 171 (1988).
6. For references to calculations and simulations of particles between two walls, see R. Kjellander and S. Sarman, *Mol. Phys.* **70**, 215 (1990).
7. J. E. Lane and T. H. Spurling, *Aust. J. Chem.* **29**, 2103 (1976); *Chem. Phys. Lett.* **67**, 107 (1979).
8. F. F. Abraham, *J. Chem. Phys.* **68**, 3713 (1979).
9. I. K. Snook and W. van Megen, *ibid.* **72**, 2907 (1980).
10. M. Schoen, D. J. Diestler, J. H. Cushman, *ibid.* **87**, 5464 (1987).
11. C. L. Rhykerd, Jr., M. Schoen, D. J. Diestler, J. H. Cushman, *Nature* **330**, 461 (1987).
12. M. Schoen, C. L. Rhykerd, D. J. Diestler, J. H. Cushman, *Science* **245**, 1223 (1989).
13. P. A. Thompson and M. O. Robbins, *Phys. Rev. A* **41**, 6830 (1991); *Science* **250**, 792 (1990).
14. M. Lupkowski and F. van Swol, *J. Chem. Phys.* **95**, 1995 (1991).
15. J. C. Maxwell, *Philos. Trans. R. Soc.* **157**, 49 (1867).
16. S. Goldstein, *Modern Developments in Fluid Dynamics* (Clarendon Press, Oxford, 1938), vol. 2, pp. 676–680.
17. Committee for the Study of Viscosity of the Academy of Sciences at Amsterdam, *Second Report of Viscosity and Plasticity* (Nordemann, New York, 1938).
18. I. Bitsanis, J. J. Magda, M. Tirrell, H. T. Davis, *J. Chem. Phys.* **87**, 1733 (1987).
19. T. K. Vanderlick and H. T. Davis, *ibid.*, p. 1791.
20. I. Bitsanis, T. K. Vanderlick, M. Tirrell, H. T. Davis, *ibid.* **89**, 3152 (1988).
21. A. I. Bailey and J. S. Courtney-Pratt, *Proc. R. Soc. A* **227**, 500 (1955).
22. J. N. Israelachvili and D. Tabor, *Wear* **24**, 386 (1973).
23. J. N. Israelachvili, P. M. McGuiggan, A. M. Homola, *Science* **240**, 189 (1988).
24. J. Van Alsten and S. Granick, *Phys. Rev. Lett.* **61**, 2570 (1988).
25. J. Peachey, J. Van Alsten, S. Granick, *Rev. Sci. Instrum.* **62**, 463 (1991).
26. D. Tabor and R. H. S. Winterton, *Proc. R. Soc. A* **312**, 435 (1969).
27. J. N. Israelachvili and G. E. Adams, *J. Chem. Soc. Faraday Trans. II* **74**, 975 (1978).
28. J. Van Alsten and S. Granick, *Langmuir* **6**, 214 (1990).
29. _____, *Macromolecules* **23**, 4856 (1990).
30. _____, *Tribol. Trans.* **33**, 436 (1990).
31. G. A. Carson, H.-W. Hu, S. Granick, *ibid.*, in press.
32. H.-W. Hu, G. A. Carson, S. Granick, *Phys. Rev. Lett.* **66**, 2758 (1991).
33. G. A. Carson, H.-W. Hu, S. Granick, unpublished experiments.
34. M. L. Gee, P. M. McGuiggan, J. N. Israelachvili, A. M. Homola, *J. Chem. Phys.* **93**, 1895 (1989).
35. A. M. Homola, J. N. Israelachvili, M. L. Gee, P. M. McGuiggan, *J. Tribol.* **111**, 675 (1989).
36. P. M. McGuiggan, J. N. Israelachvili, M. L. Gee, A. M. Homola, *Mater. Res. Soc. Symp. Proc.* **140**, 79 (1989).
37. A. M. Homola, J. N. Israelachvili, P. M. McGuiggan, M. L. Gee, *Wear* **136**, 65 (1990).
38. A. M. Homola, H. V. Nguyen, G. Hadziioannou, *J. Chem. Phys.* **94**, 2346 (1991).
39. J. Van Alsten and S. Granick, *Tribol. Trans.* **32**, 246 (1989).
40. See appendix of H.-W. Hu and S. Granick, *Macromolecules* **23**, 613 (1990); also see appendix of (25).
41. M. Vacatello, D. Y. Yoon, B. C. Laskowski, *J. Chem. Phys.* **93**, 779 (1990).
42. M. W. Ribarsky and U. Landman, *ibid.*, in press.
43. J. D. Ferry, *Viscoelastic Properties of Polymers* (Wiley, New York, ed. 3, 1980).
44. J. Koplik, J. R. Banavar, J. F. Willemsen, *Phys. Rev. Lett.* **60**, 1282 (1988).
45. W. Philippoff, *Trans. Soc. Rheol.* **10**, 317 (1966).
46. J. D. Ferry, private communication.
47. T. Vardag, F. Bachl, S. Wappman, H.-D. Lüdemann, *Ber. Bunsenges. Phys. Chem.* **94**, 336 (1990).
48. B. J. Alder and T. E. Wainwright, *Phys. Rev. A* **1**, 18 (1970).
49. G. P. Morriss and D. J. Evans, *ibid.* **32**, 2425 (1985).
50. A. J. C. Ladd, W. E. Alley, B. J. Alder, *J. Stat. Phys.* **48**, 1147 (1987).
51. For a review, see D. R. Nelson, *Phase Transitions* **7**, 1 (1983).
52. J. Douglas, private communication.
53. J. P. Rabe and S. Buchholz, *Phys. Rev. Lett.* **66**, 2096 (1991).
54. For a review, see K. J. Strandburg, *Rev. Mod. Phys.* **60**, 161 (1988).
55. G. Carson and S. Granick, *J. Mater. Sci.* **5**, 1745 (1990).
56. C. Kessel and S. Granick, *Langmuir* **7**, 532 (1991).
57. C. E. D. Chidsey, G.-Y. Liu, P. Rowntree, G. Scoles, *J. Chem. Phys.* **91**, 4421 (1989).
58. D. Y. C. Chan and R. G. Horn, *ibid.* **83**, 5311 (1985).
59. J. N. Israelachvili, *J. Colloid Interface Sci.* **110**, 263 (1986).
60. J. Van Alsten, S. Granick, J. N. Israelachvili, *ibid.* **125**, 739 (1988).
61. R. G. Horn, S. J. Hirz, G. Hadziiouannou, C. W. Frank, J. M. Catala, *J. Chem. Phys.* **90**, 6767 (1989), and references therein.
62. C. L. Jackson and G. B. McKenna, *ibid.* **93**, 9002 (1990).
63. _____, *J. Non-Cryst. Solids* **131–133**, 221 (1991).
64. B. G. Silbernagel, A. R. Garcia, J. M. Newsam, R. Hulme, *J. Phys. Chem.* **93**, 6506 (1989).
65. J. Warnock, D. D. Awschalom, M. W. Shafer, *Phys. Rev. B* **34**, 475 (1986).
66. _____, *Phys. Rev. Lett.* **57**, 1753 (1986).
67. D. D. Awschalom and J. Warnock, *Phys. Rev. B* **35**, 6779 (1987).
68. M. Mackowiak, G. Liu, J. Jonas, *J. Chem. Phys.* **93**, 2154 (1990).
69. J. Tabony and J. P. Korb, *Mol. Phys.* **56**, 1281 (1985).
70. J. P. Korb, M. Winterhalter, H. M. McConnell, *J. Chem. Phys.* **80**, 1059 (1984).
71. G. Liu, M. Mackowiak, Y. Li, J. Jonas, *Chem. Phys.* **149**, 165 (1990).
72. P. A. Thompson and M. O. Robbins, *Phys. Rev. Lett.* **63**, 766 (1989).
73. I. Bitsanis, S. A. Somers, H. T. Davis, M. Tirrell, *J. Chem. Phys.* **93**, 3427 (1990).
74. J. Klein, D. Perahia, S. Warburg, *Nature* **352**, 143 (1991).
75. It is a privilege to acknowledge the contributions of outstanding co-workers: J. Van Alsten, G. Carson, H.-W. Hu, and J. Peachey. I am grateful to J. Douglas, J. D. Ferry, N. M. Kostić, K. Schweitzer, and F. van Swol for thoughtful criticisms of a draft of this manuscript. Supported by the U.S. National Science Foundation through the Tribology Program and through the Materials Research Laboratory at the University of Illinois.